Hyperfine Interact (2017) 238:69
https://doi.org/10.1007/s10751-017-1437-3

Iron state in iron nanoparticles with and without zirconium

V. P. Filippov[1] · A. M. Khasanov[2] · Yu. A. Lauer[1]

Abstract Mössbauer and X-ray methods are used for investigations of structure, stability and characteristics of pure-iron grain and two iron-zirconium alloys such as Fe + 5 wt.% Zr and Fe + 10 wt.% Zr. The used powder was ground for 24 h in a SPEX Model 8000 mill shaker. Complex nanoparticles are found, which change their properties under milling. Mössbauer spectral parameters are obtained for investigated materials. Milling results in formation of nanosized particles with two states of iron atoms: one main part is pure α-Fe and another part of iron atoms displaced in grain boundaries or defective zones in which hyperfine magnetic splitting decrease to $\sim$30.0 T. In alloys with Zr three iron states are formed in each alloy, main part of iron is in the form of α-Fe and another two states depend on the concentration of Zr and represent iron in grain boundaries with Zr atoms in nearest neighbor. The changing of iron states is discussed.

Keywords Mössbauer spectroscopy · Zirconium alloys · Nanoparticles of Fe and Zr-Fe alloys · Milling

This article is part of the Topical Collection on *Proceedings of the 3rd Mediterranean Conference on the Applications of the Mössbauer Effect (MECAME 2017), Jerusalem, Israel, 5–7 June 2017*
Edited by Mira Ristić, Stjepko Krehula, Israel Nowik and Israel Felner

✉ V. P. Filippov
vpfilippov@mephi.ru

[1] National Research Nuclear University MEPhI (Moscow Engineering Physics Institute), 31 Kashirskoe shosse, 115409, Moscow, Russia

[2] University of North Carolina - Asheville, One University Heights, Asheville, NC 28804, USA

Published online: 09 October 2017

1 Introduction

Zirconium alloys have found a wide application in engineering. Alloys are used both with a low iron content, as well as with an increased content, where zirconium enters as a doping additive. To obtain the necessary properties of the alloys, alloying elements are added therein and thermomechanical treatments are carried out. In zirconium alloys, precipitates are formed, which can be various intermetallic compounds of complex and variable composition. The crystal size plays a very important role in the mechanical properties of alloys. For many materials, the yield strength, σ_y, varies with average grain size according to the Hall-Petch equation [1]:

$$\sigma_y = \sigma_0 + kd^{-\frac{1}{2}} \tag{1}$$

where d is the grain diameter and σ_0 and k are material specific constants.

High-energy mechanical ball milling has been widely used to prepare nanocrystalline metallic materials. The crystalline-to-nancrystalline transformation evolves a host of modifications and enhancements in properties that have wide applications in science, engineering and medicine. In order for successful application of nanocrystalline materials in industry the nano-ordered iron lattice must be stabilized. The premise of this work is to demonstrate that, in iron, grain size stability in the nanocrystalline regime is greatly influenced by grain boundary energy. Impurity additions such as zirconium that do not dissolve readily in solid solution may lower grain boundary energy and, thus, promote stability of the nanocrystalline structure. For many polycrystalline materials, the grain size varies with annealing time (time at elevated temperature) according to the relationship [2, 3]:

$$D^{1/n} - D_0^{1/n} = kt \tag{2}$$

where D is average grain diameter after annealing for time t, D_0 is initial grain diameter ($t = 0$), and n, k are temperature dependent rate constants.

In some instances, under ideal conditions, the value of n is taken to be 0.5 and the above equation describing grain growth is written as:

$$D^2 - D_0^2 = kt \tag{3}$$

The rate constant k, in the above equation can be expressed as an Arrhenius-type equation:

$$k = k_0 \exp\{-Q/RT\} \tag{4}$$

where Q is the activation energy for isothermal grain growth, k_0 is pre-exponential constant, R is gas constant, 8.31 J/mol-K and T is absolute temperature (K). The activation energy term, Q is often used to identify the dominant mechanism of grain growth.

2 Experimental procedure

The iron powder (99.9% pure) with approximate particle size of < 75 μm and zirconium powder (98% pure) with approximate similar particle size was loaded into an ampule of tool steel in an atmosphere of pure argon with balls of 6.4 and 7.9 mm diameter, 440 °C into a mill with ball bearings in stainless steel and the ratio of the weight of the balls to the weight of the powder equal to 10:1. The initial weight of the sample charge was 5 g. Thus, the behavior of the growth of pure-iron grain and two iron-zirconium alloys (Fe+5 wt.% Zr and Fe+10 wt.% Zr) is investigated. The used powder was ground for 24 h in a SPEX Model 8000 mill shaker, which was cooled to a temperature of approximately 50 °C.

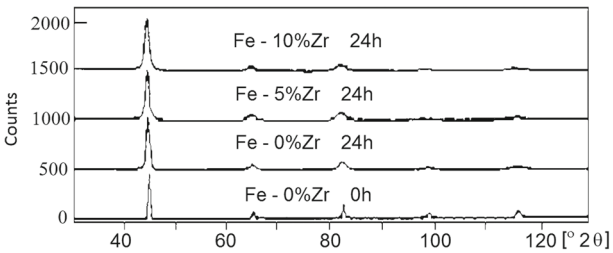

Fig. 1 *X*-ray diffraction patterns of pure iron before and after milling and doped iron after milling. Broader peaks in the doped samples are indicative of smaller grain size

Samples were annealed in an inductive box furnace and in a pure argon atmosphere for times ranging from some minutes to 4 h at 725 K and 825 K.

X-ray diffraction (XRD) was performed on the as-milled and annealed samples with a Philips X-pert diffractometer and CuKα radiation ($\lambda = 1.54$ Å) at 100 steps per degree and a count time of 2.5 to 5 s per step. Reflections from the five most intense peaks of iron (from the 110, 200, 211, 220 and 310 planes) were used to calculate grain size using the full width at half maximum (FWHM) measurement incorporated into the Scherrer formula below:

$$t = K\lambda((Bcos\theta)^{-1} \tag{5}$$

where θ is the Bragg angle, λ is the wavelength of the X-ray, t is the crystal particle size, B is the FWHM after correcting diffractometer broadening, and K is a unit cell geometry dependent constant whose value is usually between 0.85 and 0.99 taken as 0.9 in this study. At study of powders, there is no need to take into account the micro deformation present in massive and most often textured materials [4].

Prior to heat treatment, ^{57}Fe Mössbauer spectroscopy and energy dispersive spectroscopy (EDS) were used to quantify structural and compositional changes following milling. ^{57}Fe Mössbauer spectroscopy measurements were made at room temperature using a constant acceleration spectrometer. A ^{57}Co source in a rhodium matrix was used for the measurements and α-Fe is used as the reference material. Pure iron samples were fit using one component while zirconium doped samples were fit using three components in the spectra. Also prior to heat treatment, energy dispersive spectroscopy was carried out to determine alloying levels and possible impurity contaminants.

3 Results and discussion

3.1 *X*-ray diffraction and thermal analysis

Figure 1 shows the X-ray diffraction patterns for the as-received iron and iron with 0.5 and 10 wt.% Zr additions after milling for 24 h. The X-ray patterns do not reveal any significant source of contamination and this is confirmed by EDS analysis which also shows the expected levels of zirconium addition. Instrumental line broadening as indicated by the XRD-pattern of the as received iron assuming large crystal size was taken into account in the determination of the grain size of the milled samples. In using the Scherrer formula in this study, the internal lattice strain, which also causes line broadening, was not accounted for.

Table 1 Average grain size for each synthesized powder as calculated by the Scherrer method

Powder	Avarage grain size, nm
Fe	16
Fe+5 wt.% Zr	12
Fe+10 wt.%Zr	11

Table 2 Final grain size after treatment as calculated by the Sherrer method

Annealing temperature, K	Time. s	Average grain size, nm		
		Fe	Fe+5%Zr	Fe+10%Zr
825	300	63	18	18
	1200	60	20	19
	3600	97	20	20
725	600	35	15	12
	3000	39	16	15
	10500	41	15	14

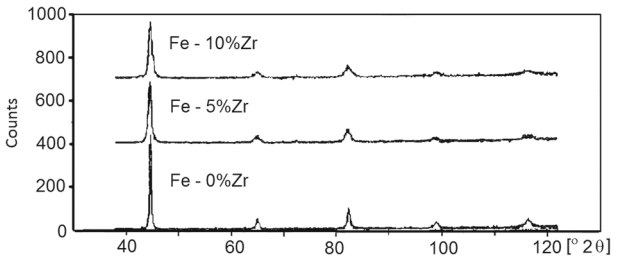

Fig. 2 X-ray patterns following heat treatment at 725 K for 10500 s (175 min). Apparent differences in the patterns suggest pure iron recrystallize much more readily

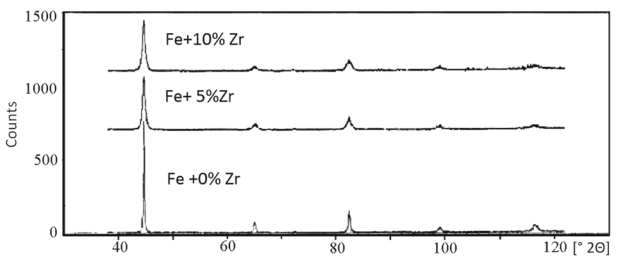

Fig. 3 X-ray patterns following heat treatment at 825 K for 3600 s (60 min). As seen in the lower temperature measurement broader lines in doped samples indicate smaller grain size

After 24 h of milling time, the grain sizes as determined using the Scherrer formula are shown in Table 1.

These grain sizes are consistent with the range of grain sizes reported in other works in the literature on similarly milled pure iron [5–8]. It is noted that the grain size stabilized after milling iron with zirconium additions is approximately 25% lower than identically milled pure iron.

One explanation is that an enhanced structural stability emergies in these smaller grain sized samples leading to a reduction of dynamic recrystallization under milling conditions.

X-ray measurements were performed on all annealed samples and the results of the Scherrer formula calculations are summarized in Table 2. A sample of the comparative line broadening is shown in the X-ray diffraction patterns for the alloy series annealed at 725 K and up to 10500 s as shown in Fig. 2, annealed at 825 K for 3600 s (60 min) as shown in Fig. 3. One can see that at 825 K the broadening is less than at 725 K that means the increasing of particle sizes which is clearly demonstrated in Table 2.

Plots of grain diameter, D, versus time show that in all materials the grain size increases rapidly after short initial annealing period, then continues to grow at a much slower rate over the longer times (Fig. 4). It is readily apparent that grain growth is inhibited significantly in the zirconium-doped nanocrystalline iron samples.

The doped alloys stabilize at a grain size of around 20 nm while the undoped iron counterpart ultimately grows to around 90 nm, indicating over 75% reduction in the final grain size observed at the highest temperature and time.

The activation energy for grain growth, Q, is deduced from an Arrhenius plot (2) shown in Fig. 5 and which gives a value of 152 kJ/mol for the pure iron. This value is close to that of the activation energy for grain boundary diffusion in iron 174 kJ/mol, suggesting this as the mechanism for grain growth. This assessment concurs with other work [6–8], which has similarly suggested that in the time and temperature regime studied here, grain growth occurs by ussested mechanism. These works show that at higher temperatures and times, the mechanism shifts to one controlled by lattice diffusion where the activation energy is around 250 kJ/mol. However, in the zirconium-doped alloys, the activation energy is less even than that for grain boundary diffusion, which is approximately 115 kJ/mol, and suggests another controlling mechanism or combination of mechanisms is at play in these Fe-Zr systems.

The significant reduction in grain growth may be explained by several reasons including the solute drag effect (Zener pinning) whereby incoherent phases that exist on grain boundaries inhibit the driving force of the boundary migration. For the boundary to move past the incoherent phase new boundary must be produced. This requires a certain amount of energy related to the grain boundary energy and can create a “pinning” pressure that restricts boundary motion at these points. Also it is possible that the presence of zirconium at the grain boundaries reduces the overall grain boundary energy. Reducing the grain boundary energy term would reduce the overall driving force for reduction of boundary area. Analysis by differential scanning calorimetry (DSC) may help to ascertain this possibility by measuring heat release of stored enthalpy. Yet another possibility may involve consideration of the increased diffusivity of iron in zirconium lattice compared to the self-diffusion of iron.

3.2 Mössbauer spectroscopy

Mössbauer spectra obtained at room temperature are shown in Figs. 6 and 7.

Spectra fitting results are given in Table 3. It is obvious that the spectral shape changes after milling and for iron-zirconim alloys with increasing of Zr content.

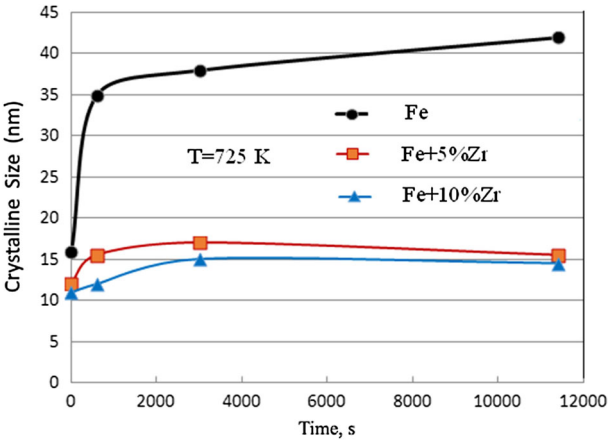

Fig. 4 Grain growth of the three powders annealed at 725 K

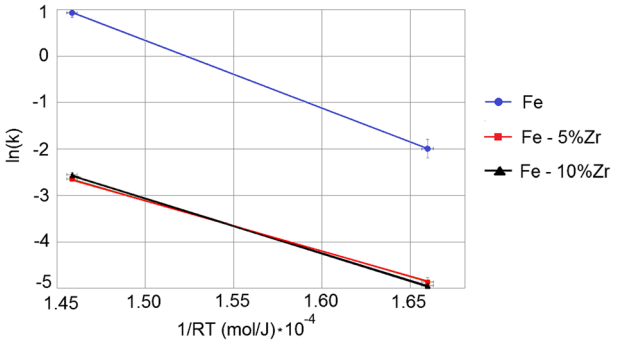

Fig. 5 An Arrhenius-style plot showing the iteration in activation energy for doped powders

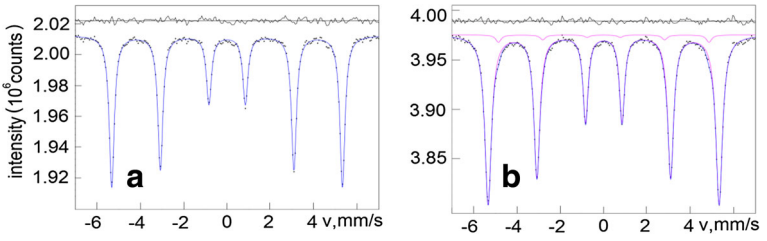

Fig. 6 ^{57}Fe Mössbauer spectra of pure iron samples as pre (**a**) and post (**b**) milling

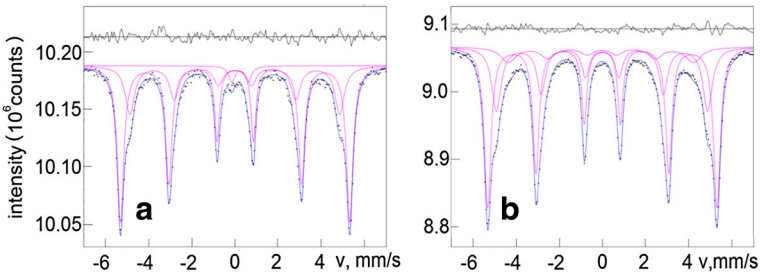

Fig. 7 ^{57}Fe Mössbauer spectra of doped samples in the amounts of 5 wt.% Zr (**a**) and 10 wt.% Zr (**b**)

Table 3 Mössbauer spectra parameters

Sampl (milling time)	Subspectra	Isomer shift (mm/s)	Quadroupole splitting (mm/s)	Magnetic splitting (T)
Fe	1	0	0	33.0
Fe (24 h)	1	0	0	33.0
	2	0	0	30.0
Fe+5% Zr (24 h)	1	0	0	32.9
	2	0	0	30.2
	3	0.26	0.74	0
Fe+10% Zr (24 h)	1	0	0	32.9
	2	0	0	30.4
	3	0	0	27.1

Mössbauer data suggests that zirconium segregates to the grain boundaries in nanocrystalline iron synthesized via high-energy ball milling. Pure iron powders were fit (Fig. 6a) with one component of hyperfine magnetic splitting (hms) ($H_{eff} = 33.0$ T) indicating that only one unique environment of iron existed in the pure iron samples, which is to be expected. Two subspectra are observed in the milled pure iron powders (Fig. 6b), indicating two separate environments of iron. One of them is that of α-Fe, the bulk of the sample. The second subspectrum ($H_{eff} = 30.0$ T) with low intensity may represent the iron located at the grain boundaries or the part of iron in the defective surface layers of nanoparticles. This conclusion is made in accord with results obtained in [5, 6]. In [5] it was shown that after milling of iron in Ar and N gasses the magnetic field splitting for the corner atoms to be slightly less than the magnetic field associated with the cell center atoms. This is due to dislocations lacated and generated at the grain boundaries, so this indicates the presence of defective zones at the grain boundaries. In defective zones the distance beetween iron atoms is increased which results in deacrese of hms. In [6] milling of pure iron and iron chromium alloys was studied. For pure iron Mössbauer spectrum becomes broad after 100 h milling. This broadening is explained by existence of extra hms in addition to hyperfine magnetic field of pure α-Fe. So, the existence of hms with $H_{eff} \sim 30.0$ T may be explained by presence of iron in defect zones.

Three subspectra are observed in the doped iron samples (Fig. 7), indicating three separate environments of iron. The most abundant of these environments is that of α-Fe, the bulk

of the sample. The second subspectrum (H_{eff} = 30.2 T) for Fe+5%Zr and (H_{eff} = 30.4 T) for Fe+10%Zr with low intensity may represent the iron particles located at the grain boundaries or/and the part of iron in the defective surface layers of nanoparticles. The intensities of this lines in zirconium containing samples are grater then that of pure iron sample (H_{eff} = 30.0 T) in pure iron sample (Fig. 6b). This second subspectrum (Fig. 7) could represent the iron particles located at the grain boundaries or the part of iron in the defective surface layers of nanoparticles as for pure iron. The presence of Zr atoms is possible too.

The third subspectrum (H_{eff} = 27.1 T) for the sample Fe+10%Zr can be explained by influence of Zr atoms in these nanoparticles.

Such explanation is made according results obtained in [7, 8]. In [7] alloys Fe+10%Zr were studied after milling processes. Ball milling in the high-energy AGO-2 mill results in the formation of supersaturated α-Fe(Zr) solid solution with Zr segregations at grain boundaries. In paper [8] the milling of Fe+20%Zr in Ar results in appearance of some hms subspectra. The main component of spectra is a sextet with parameters H_{eff} = 33.0 T which corresponds to the particles with bcc α-Fe structure. The spectra also contain components–sextets with magnetic hyperfine field values lower than for bcc α-Fe: 30.3, 29.8, 27.8 and 24.0 T. These components were interpreted in [9] as iron in crystalline phase and a disordered state with Zr atoms present in the grain boundary of nanocrystalline (nc) iron, according to which a spectrum of nc iron is described by the component corresponding to the grain of iron crystalline phase and by components which are due to the disordered state with the presence of Zr atoms in the grain boundary zone of the nanocrystalline iron.

The subspectrum of paramagnetic phase (Fig. 7a) with IS = 0.26 mm/s and QS = 0.74 mm/s can't be explained correctly at this stage of investigations. One can hypothesize iron diffused into the grain boundary with high concentration of Zr displays superparamagnetic properties [9, 10].

Analyzing of spectra parameters shows that there are no parameters of known intermetallic compounds such as $ZrFe_2$ or Zr_3Fe or Zr_2Fe. It means the milling in such conditions doesn't follows by formation of known intermetallic compounds.

4 Conclusions

1. The structural stability and grain growth of nanocrystalline iron and iron with minor additions of zirconium were investigated.
2. It was shown that:
   a) Grain growth in the studied iron-zirconium alloys is observed to be significantly slower and stabilizes at a much smaller size than the pure iron counterpart.
   b) Rate constants for grain growth are lower in the alloyed material than pure iron and the activation energy for growth is also lower. This suggests that a different mechanism or combination of mechanisms controls crystal growth in these systems.
3. Intermetallic Zr-Fe compounds are not detected during nanosized particles formation by milling.
4. It appears that the ability to introduce impurities to form complex (possibly multicomponent) nanocrystalline metal systems may offer a promising route for processing a new breed of engineering materials that can offer exceptional mechanical properties.

Acknowledgements This study was supported by MEPhI's competitive program.

References

1. Malow, T.R., Koch, C.C.: Grain growth in nanocrystalline ion prepared by mechanical attrition. Acta Mater. **45**(5), 2177–2186 (1997)
2. Murty, B.S., Datta, M.K., Pabi, S.K.: Structure and thermal stability of nanocrystalline materials. Sadhana **28**(1–2), 23–45 (2003)
3. Del Bianko, L., Hernando, A., Bonetti, E.: Grainboundary structure and magnetic behavior in nanocrystalline ball-milled iron. Phys. Rev. B **56**(14), 8894–8901 (1997)
4. Perlovich, Yu.., Isaenkova, M., Bunge, H.J.: The fullest description of the structure of textured metal materials with generalized pole figures: the example of rolled Zr alloys. Mater. Sci. Forum **378–381**, 180–185 (2001)
5. Ravers, J., Cook, D., Tae, K.: X-ray difraction and Mössbauer characterisation of attrition-milled nanostructured iron and iron-nitrogen powders. Philos. Mag. A **78**(4), 965–977 (1998)
6. Murugesan, M., Kuwano, H.: Magnetic properties of nano-crystalline Fe-Cr alloys prepared by mechanical alloying. IEEE Trans. Magnet. **35**(5), 3499–3501 (1999)
7. Kwon, Y.S., Kim, J.S., Povstugar, I.V., Yelsukov, E.P.: Role of local heating in crystallization of amorphous alloys under ball milling: an experiment on Fe90Zr10. Phys. Rev. B **75**, 144112-6 (2007)
8. Kiseleva, T.Yu.., Letsko, A.I., Talako, T.L., et al.: Mechanochemically synthesized powder precursors local structure influence on the microstructure of SHS Fe2O3/Fe/Zr/ZrO2 composites. Nanotechnol. Russ. **10**(3–4), 220–230 (2015)
9. Rixecker, G.: Mössbauer spectroscopic studies of defect structure alloying effects in nanostructured materials. Hyper. Interact. **130**, 127–150 (2000)
10. Kiseleva, T.Y., Novakova, A.A.: Mössbauer spectroscopy in the technology of nanocomposite functional materials. Bull. Russ. Acad. Sci. Phys. **79**(8), 1002–1008 (2015)